13. Yu. B. Kolesnikov and A. B. Tsinober, Izv. Akad. Nauk SSSR, Mekh. Zhidk. Gaza, No. 4, 146-150 (1974).
14. S. Sukoriansky and H. Branover, Progress in Astronautics and Aeronautics, 112, 87-99 (1988).

KINETICS OF HEAT TRANSFER TO A SPHERICAL PARTICLE FROM A RAREFIED PLASMA. 3. MAXWELLIAN ION APPROXIMATION

A. G. Gnedovets, A. V. Gusarov, and A. A. Uglov

UDC 533.9

The authors describe the kinetics of heat transfer to a spherical particle from a rarefied plasma with a Maxwellian velocity distribution of molecules, electrons, and ions.

A material particle in a rarefied plasma experiences collisions with molecules, electrons, and ions, resulting in transfer of energy and charge. Plasma electrons recombine on the surface and are absorbed by the particle, and the ions are neutralized by electrons of the material and scattered by the particle surface in the same manner as are incident molecules of the plasma gas. It is important that due to the large difference in the thermal velocities of electrons and plasma ions the particle acquires a negative potential $\varphi_f < 0$ for which the electron and ion charge flux compensate each other, $J_e^-(\varphi_f) = J_i^-(\varphi_f)$. During collisions of electrons and ions with the surface, besides kinetic energy the particle receives energy of the charged states corresponding to the work function Φ_e and the effective ionization energy $I_i - \Phi_e$.

Computations of heat transfer between the particle and the plasma reduce to determining the number flux of plasma particles $J_j^\pm$ of each type and the kinetic energy $E_j^\pm$ transferred by them, from simultaneous solution of the kinetic Boltzmann–Vlasov equation for the velocity distribution function f_j and the Poisson equation for the potential $\varphi(r)$. The main complications in solving the kinetic problem are linked to describing the motion of ions in the attractive field of a charged particle. This arises from the use of simplified distribution models, e.g., the cold ion [1] and the monoenergetic ion [2] approximations, used to describe heat transfer to a particle in [3, 4]. Therefore, it is of interest to analyze beat transfer to a spherical particle from a collisionless plasma at rest ($\ell_j \gg R$) in the more realistic case when the ions, as well as the molecules and electrons, are subject to a Maxwellian velocity distribution in the unperturbed plasma region far from the particle:

$$f_{j\infty} = N_{j\infty} \left(\frac{m_j}{2\pi k T_{j\infty}} \right)^{3/2} \exp\left(-\frac{m_j v^2}{2kT_{j\infty}} \right). \quad (1)$$

For a diffuse law of scattering of molecules and neutralized ions by the particle surface in conditions when thermal-emission processes are not important, the relations for the heat flux $q_j = Q_j/E_j^0$ for each type of plasma particle in dimensionless form are as follows:

$$q_a = 1 - \tau_s, \quad (2)$$

$$q_e = e_e^- + \frac{1}{2} j_e^- w_e, \quad (3)$$

$$q_i = e_i^- + j_i^- \left(\frac{1}{2} w_i - \tau_s \right), \quad (4)$$

A. A. Baikov Metallurgical Institute, Russian Academy of Sciences, Moscow. Translated from Inzhenerno-fizicheskii Zhurnal, Vol. 62, No. 2, pp. 254-260, February, 1992. Original article submitted April 29, 1991.

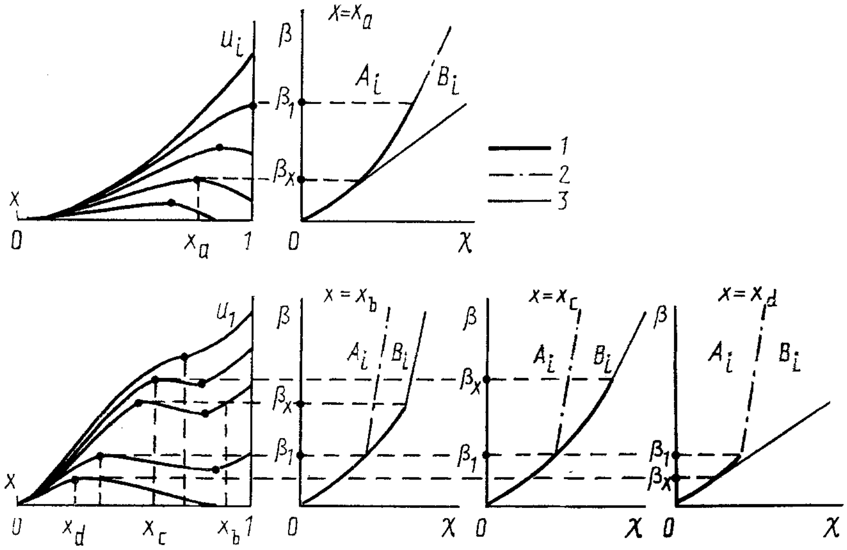

Fig. 1. Distributions of effective potential $u_i(x)$ for various values of χ and possible β—χ phase space configurations of plasma ions at different distances x from the particle: A_i, B_i) ions with trajectories intersecting and not intersecting the particle surface; boundaries of the regions: 1) $\chi = G_m(\beta)$; 2) $\chi = G_1(\beta) = 2(\beta + \tau y_f)$; 3) $\chi = G_x(\beta) = 2(\beta + \tau y)/x^2$.

where $j_j^- = J_j^-/J_j^0$; $e_j^- = E_j^-/E_j^0$; $w_j = W_j/kT_{j\infty}$; $\tau_s = T_s/T_{h\infty}$; $W_e = \Phi_e$; $W_i = I_i - \Phi_e$; $J_j^0 = N_{j\infty}(kT_{j\infty}/2\pi m_j)^{1/2}$; $E_j^0 = N_{j\infty}kT_{j\infty}(2kT_{j\infty}/\pi m_j)^{1/2}$.

The electron fluxes are determined only by the particle potential $y_f = -e\varphi_f/kT_{e\infty}$ and are computed to be

$$j_e^- = \exp(-y_f), \quad e_e^- = \exp(-y_f). \tag{5}$$

The fluxes of charge and energy carried by the ions depend on the spatial distribution of potential in the plasma, determined by solving the Poisson equation. Reference [3] formulated the problem and gave relations for the distribution of electron density in the vicinity of the particle.

The ion transport processes have been described from analysis of their possible trajectories in [2, 5], where the chosen integrals of the motion were the total energy $\mathscr{E} = (1/2)\times m_i(v_r^2 + v_t^2) + e\varphi(r)$ and the momentum $\Omega = m_i r v_t$. The densities, ion fluxes, and the transferred energy, as is true for any other macroscopic characteristics, are represented as moments of the distribution function over the "energy—momentum" phase space. The topology of the β—χ phase space is determined by the behavior of the effective potential $u_i(x) = -\tau y(x) + (1/2)x^2\chi$, which plays the role of a potential barrier for ions ($\beta = \mathscr{E}/kT_{i\infty}$, $\chi = \Omega^2/m_i R^2 kT_{i\infty}$, $y = -e\varphi/kT_{e\infty}$, $x = R/r$, $\tau = T_{e\infty}/T_{i\infty}$). In the β—χ phase plane one can identify two regions corresponding to ions of different classes: A_i, populated by ions whose trajectories intersect the particle surface; and B_i, populated by ions whose trajectories bypass the particle. The region boundaries are formed by the straight lines $\chi = G_1(\beta) = 2(\beta + \tau y_f)$, $\chi = G_x(\beta) = 2(\beta + \tau y)/x^2$ and the curve $\chi = G_m(\beta)$, determined by the position of the maximum effective potential and given parametrically as $\beta = -\tau y(x') + (1/2)x'^2\chi$, $\chi = (\tau/x')(dy/dx')$. Two variants are possible, depending on the particle size and the nature of the spatial variation of electrostatic potential in the plasma: 1) for any χ the effective potential $u_i(x)$ has no more than one local extremum, a maximum; 2) no more than two extrema, a maximum and a minimum. The possible topological structures of the β—χ space and its relationship to the distribution of the effective potential $u_i(x)$, in which χ varies as a parameter, are shown in Fig. 1.

The dimensionless distribution functions $\hat{f}_i^\pm = f_i^\pm/[N_{i\infty}(m_i/2\pi kT_{i\infty})^{3/2}]$ of the incident ($v_r < 0$) and reflected ($v_r \geq 0$) ions, as follows from the Boltzmann—Vlasov equation, are represented in the form $\hat{f}_i^\pm = n_K^\pm \exp(-\beta)$, where the subscript K denotes the region of phase space. Since the ions are neutralized on the surface, we have $n_{A_i}^- = n_{B_i}^- = 1$, $n_{A_i}^+ = 0$, $n_{B_i}^+ = 1$. Therefore, the dimensionless densities $n_i = N_i/N_{i\infty}$ and fluxes j_i^- and e_i^- are computed as:

$$n_i = \frac{\pi x^2}{(2\pi)^{3/2}} \iint\limits_{A_i+B_i} \frac{\nu_K \exp(-\beta)\, d\beta d\chi}{[2(\beta+\tau y) - x^2\chi]^{1/2}}, \tag{6}$$

$$j_i^- = \frac{1}{2} \iint\limits_{A_i} \exp(-\beta)\, d\beta d\chi, \tag{7}$$

$$e_i^- = \frac{1}{4} \iint\limits_{A_i} (\beta + \tau y_f) \exp(-\beta)\, d\beta d\chi, \tag{8}$$

where $\nu_{A_i} = 1$, $\nu_{B_i} = 2$. Integration leads to the formulas:

$$n_i(x) = F(\beta_1) - H_\beta(0, \beta_x) + H_\beta(\beta_x, \beta_1), \tag{9}$$

$$j_i^- = (1 + \beta_1 + \tau y_f) \exp(-\beta_1) + \frac{1}{2} \int_0^{\beta_1} G_m(\beta) \exp(-\beta)\, d\beta, \tag{10}$$

$$e_i^- = \frac{1}{2} [1 + (1 + \beta_1 + \tau y_f)^2] \exp(-\beta_1) + \frac{1}{4} \int_0^{\beta_1} (\beta + \tau y_f) G_m(\beta) \exp(-\beta)\, d\beta. \tag{11}$$

Here

$$F(\beta) = \frac{1}{2} \operatorname{erfc}(\tau y)^{1/2} \exp(\tau y) +$$

$$+ \frac{1}{2}(1 - x^2)^{1/2} \operatorname{erfc}\left(\beta + \frac{\tau(y - x^2 y_f)}{1 - x^2}\right)^{1/2} \exp\left(\frac{\tau(y - x^2 y_f)}{1 - x^2}\right) +$$

$$+ \frac{1}{\pi^{1/2}} \left[(\tau y)^{1/2} + (1 - x^2)^{1/2} \left(\beta + \frac{\tau(y - x^2 y_f)}{1 - x^2}\right)^{1/2} \exp(-\beta)\right],$$

$$H_\beta(a, b) = \frac{1}{(2\pi)^{1/2}} \int_a^b [2(\beta + \tau y) - x^2 G_m(\beta)]^{1/2} \exp(-\beta)\, d\beta.$$

The parameters β_x and β_1 are defined by the points of intersection (or tangency) of the curve $G_m(\beta)$ with the lines $G_x(\beta)$ and $G_1(\beta)$, respectively.

In the computations it is convenient not to use integrals with respect to the energy β, but rather with respect to the spatial coordinate $x' = R/r'$. Substitution by the variable $\beta = g(x') = -\tau y(x') + (1/2)\tau x' dy/dx'$ allows us finally to write, instead of Eqs. (9)-(11):

$$n_i(x) = F(g(x_1)) - H_{x'}(0, x_*) + H_{x'}(x_*, x_1), \tag{12}$$

$$j_i^- = (1 + g(x_1) + \tau y_f) \exp(-g(x_1)) + \\ + \frac{1}{4} \tau^2 \int_0^{x_1} \frac{1}{x'} \frac{dy}{dx'} \left(x' \frac{d^2 y}{dx'^2} - \frac{dy}{dx'}\right) \exp(-g(x'))\, dx', \tag{13}$$

$$e_i^- = [1 + (1 + g(x_1) + \tau y_f)^2] \exp(-g(x_1)) + \\ + \frac{1}{8} \tau^2 \int_0^{x_1} \frac{1}{x'} \frac{dy}{dx'} \left(x' \frac{d^2 y}{dx'^2} - \frac{dy}{dx'}\right) [g(x') + \tau y_f] \exp(-g(x'))\, dx', \tag{14}$$

where

$$H_{x'}(a, b) = \frac{\tau^2}{2(2\pi)^{1/2}} \int_a^b \left(x' \frac{d^2 y}{dx'^2} - \frac{dy}{dx'}\right) \left[2[y(x) - y(x')] + \frac{(x'^2 - x^2)}{x'} \frac{dy}{dx'}\right]^{1/2} \exp(-g(x'))\, dx'.$$

The limits of integration in Eqs. (9)-(14) are determined as follows: $\beta_1 = g(x_1)$; $\beta_x = g(x_*)$; x_1 and x_* are the smallest roots of the equations $(1 - x'^2) dy/dx' = 2x'[y_f - y(x')]$, $(x^2 - x'^2) dy/dx' = 2x'[y(x) - y(x')]$, written relative to x', respectively.

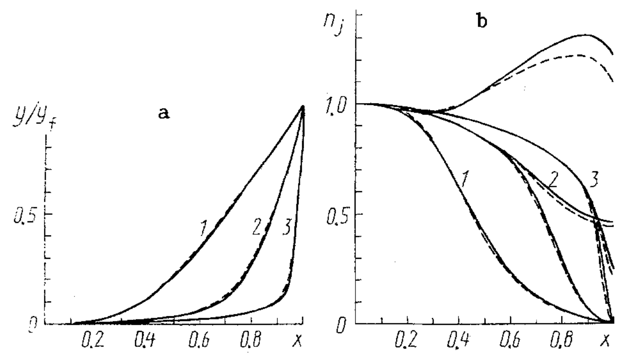

Fig. 2. Spatial distributions: a) of the potential y/y_f; b) of densities of charge carriers n_j in the particle vicinity in a one-temperature ($\tau = 1$) argon plasma; values of n_i are the top branches of the density curves, and n_e are the lower; the solid lines are Maxwell ions, and the broken lines are monoenergetic ions; 1) $x_D = 1$, $y_f = 4.04$ (4.15); 2) 0.1 and 4.51 (4.51); 3) 0.01 and 5.00 (5.02). The values in brackets are the particle potential in the monoenergetic ion approximation.

The spatial potential distribution $y = y(x)$ is found numerically by the method of successive approximations, in an analogous way to what was done in [5]. The iterative process is built on the scheme

$$y_{N+1} = \alpha_1 \tilde{y}_{N+1} + (1 - \alpha_1)\, y_N. \tag{15}$$

Here $\tilde{y}_{N+1}$ is the soluton of the Poisson equation

$$\frac{d^2 \tilde{y}_{N+1}}{dx^2} = \frac{1}{x_D^2 x^4}(n_{iN} - n_{eN}) \tag{16}$$

with the boundary conditions

$$\tilde{y}_{N+1}(0) = 0, \quad \tilde{y}_{N+1}(1) = y_N(1) + \alpha_2 \left[(\tau/\mu)^{1/2} j_{eN}^- - j_{iN}^-\right], \tag{17}$$

where $\mu = m_e/m_i$, $x_D = r_D/R$, $r_D = (kT_{e\infty}/4\pi e^2 N_{e\infty})^{1/2}$. The parameters α_1 and α_2 are chosen so as to make the iterative process converge. The densities n_{jN} and fluxes j_{jN}^- are found by substituting y_N into Eqs. (12) and (13) for ions and into the corresponding expressions for electrons [3]. As an initial approximation we can use an arbitrary monotonic increasing function $y_0(x)$ satisfying the boundary condition $y_0(0) = 0$. The boundary condition (17) on the particle surface ($x = 1$) is assigned such that equality is established during the iterative process between the electron and ion fluxes

$$j_e^- = (\mu/\tau)^{1/2}\, j_i^-. \tag{18}$$

Figures 2 and 3 show results of numerical computations of the processes of transfer of charge and energy to a spherical particle in a one-temperature ($\tau = T_{e\infty}/T_{i\infty} = 1$) argon plasma for the Maxwell ion approximation, compared with data obtained for monoenergetic ions [4]. The influence of screening properties of the plasma on the spatial distribution of potential and charge carrier densities is shown in Fig. 2. Figure 3 shows the dependence on the Debye screening parameter $x_D = r_D/R$ of the dimensionless particle floating potential $y_f = -e\varphi_f/kT_{e\infty}$ and the fluxes of charge $j_j^* = J_j^-/J^*$ and energy $e_j^* = E_j^-/E^*$ of the electrons and ions [$J^* = N_{e\infty}(kT_{e\infty}/2\pi m_i)^{1/2}$, $E^* = N_{e\infty}kT_{e\infty}(2kT_{e\infty}/\pi m_i)^{1/2}$]. An increase of x_D leads to stronger penetration of the electric field of the charged particle into the plasma and to growth of the flux of attracted ions. Since the total flux of charge to the particle must remain equal to zero, the floating particle potential falls in absolute value, to achieve the required increase of electron flux. The fluxes of energy transferred by electrons and ions also increase here.

In a region with Debye radii that are very small or large compared with the particle size the electron and ion fluxes are weakly connected with the nature of the spatial variation of potential in the plasma and are determined only by the particle floating potential.

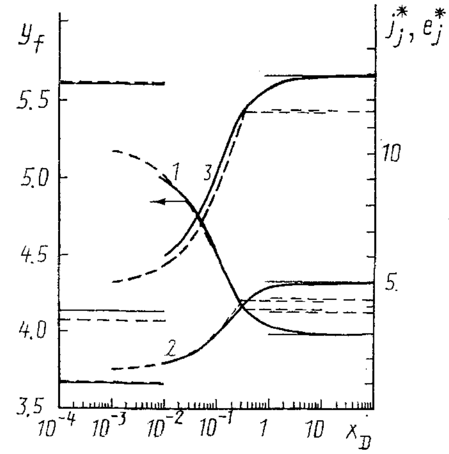

Fig. 3. Dependences of the dimensionless particle floating potential y_f and of the fluxes of charge j_j^* and energy e_j^* of electrons and ions of a one-temperature argon plasma ($\tau = 1$) on the Debye screening parameter ($x_D = r_D/R$): the solid lines are Maxwell ions, and the broken lines are monoenergetic ions; the horizontal lines are limiting values in a strongly screened and weakly screened plasma: 1) y_f; 2) $j_i^* = j_e^* = e_e^*$; 3) e_i^*.

The first case corresponds to a regime of strong plasma screening (a particle with a thin layer of space charge), and the second case corresponds to a regime of weak screening (particle with a thick layer of space charge). In both cases the particle potential and the charge and energy fluxes are practically independent of the Debye screening parameter x_D. In these limiting regimes for the Maxwell ion approximation one can obtain the analytical relations

$$j_e^* = j_i^* = e_e^* = 1/\tau^{1/2}, \quad e_i^* = \frac{1}{\tau^{3/2}}\left(1 + \frac{1}{2}\tau y_f\right), \quad y_f = -\frac{1}{2}\ln(\mu/\tau)$$

– for strong screening ($x_D \ll 1$);

$$j_e^* = j_i^* = e_e^* = \frac{1}{\tau^{1/2}}(1 + \tau y_f),$$

$$e_i^* = \frac{1}{\tau^{3/2}}\left[1 + \tau y_f + \frac{1}{2}(\tau y_f)^2\right], \quad \exp(-y_f) = (\mu/\tau)^{1/2}(1 + \tau y_f)$$

– for weak screening ($x_D \gtrsim 1$).

In a one-temperature argon plasma ($\tau = 1$) for the Maxwell ion approximation the limiting values listed are: $y_f \simeq 5.60$; $e_e^* \simeq 1$; $e_i^* \simeq 3.80$ for $x_D \ll 1$ and $y_f \simeq 3.99$; $e_e^* \simeq 4.99$; $e_i^* \simeq 12.95$ for $x_D \gtrsim 1$.

The results of calculated heat transfer from the plasma to the particle, obtained for Maxwell ions and for the simplified approximation of monoenergetic ions [4] are quite close. The dependences of the particle potential and the fluxes on Debye radius in the Maxwell ion case are smoother, and there are no bends on the corresponding curves, which results from allowing thermal scatter of the plasma ion velocities. The differences between the intensities of the electron and ion fluxes computed with the two ion distribution models are more noticeable in the weak screening region ($x_D \gtrsim 1$), but do not exceed ~15% for $\tau = 1$. Therefore, for preliminary calculations one can use the less laborious approximation of monoenergetic ions, for which the Poisson equations reduce to an ordinary differential equation, not to an integrodifferential one, as it does in the ion model considered with Maxwellian velocity distribution.

The analysis performed shows that the heat transfer is substantially influenced by the charge transfer process, particle electrification, and the nature of the screening of the particle electric field by the plasma. Since $q_i + (\tau/\mu)^{1/2}q_e \gg q_a \simeq 1$, the contribution of electrons and ions to the total heat balance is considerable, even in a plasma with a low ionization level. The role of plasma processes in the heat transfer is more apparent for particles of small size ($R < r_D$) because of the strong influence of the local particle electric field on the motion of the electrons and ions.

NOTATION

e, charge of the electron; $\mathcal{E}$, total energy; $E_j^{\pm}$, flux density of kinetic energy; I_i, ionization energy; $J_j^{\pm}$, number flux density of particles in the plasma; k, Boltzmann constant; ℓ_j, mean free path; m_j, mass; N_j, computed number density; p, pressure; Q_j, heat flux; r, spatial coordinate; r_D, Debye radius; R, particle radius; T_j, temperature; φ, plasma potential; φ_f, particle floating potential; Φ_e, electron work function; Ω, momentum. Subscripts: a, molecules; e, electrons; i, ions; h, heavy plasma particles (molecules and ions); r, radial component; s, surface; t, tangential component; ∞, unperturbed plasma region far from the particle; +(−), direction away from (toward) the particle.

LITERATURE CITED

1. J. E. Allen, R. L. F. Boyd, and P. Reynolds, Proc. Phys. Fluids, No. 2, 212-216 (1959).
2. I. B. Bernstein and I. N. Rabinowitz, Phys. Fluids, 2, No. 2, 2150-2167 (1959).
3. A. G. Gnedovets, A. V. Gusarov, and A. A. Uglov, Inzh.-fiz. Zh., 62, No. 1, 41-46 (1992).
4. A. G. Gnedovets, A. V. Gusarov, and A. A. Uglov, Inzh.-fiz. Zh., 62, No. 1, 47-50 (1992).
5. J. Laframboise, Rarefied Gas Dynamics, J. H. Leeuw (ed.), Vol. 2, Academic Press, New York—London (1966), pp. 22-44.

ENERGY CHARACTERISTICS OF A SOLID-STATE LASER PUMPED BY EMISSION FROM A CUMULATIVE JET

M. Kh. Vergasov, A. F. Leonov, N. A. Makarovets, and Yu. A. Torfimov

UDC 662.017.224.2

Optical pumping of solid-state lasers by strong shock waves formed during gas cumulation is shown to be feasible.

The possibility in principle of using strong shock waves in gases as a high-temperature high-power radiator was substantiated long ago. High radiation fluxes in small devices can be obtained by using condensed explosives (EXP) to produce strong shock waves in dense gases.

Explosive charges in a cylindrical cumulative channel are used to obtain strong shock waves in gases. A cumulative jet in the channel of such charges is formed when the detonation products collapse (gas cumulation).

It was shown in [1] that the jet velocity u is related to the detonation velocity v by

$$\frac{n^2}{n^2-1} = (x-1)^2 + \frac{n^2}{n^2-1}\left(\frac{2}{\gamma+1}\right)^{\frac{1}{n}}\left[(\gamma+1)\frac{\rho_0}{\rho\,\mathrm{exp}}\right]^{\frac{n-1}{n}} x^{\frac{2n-2}{n}}, \quad (1)$$

where $x = u/v$; ρ_0 is the initial gas density; and $P = A\rho^n$.

The given solution gives a fairly correct description of the detonation processes in a charge of limited size. After initiation the detonation wave reaches the bottom of the charge channel and initiates a shock wave in the gas. As a result of the subsequent collapse of the detonation products a jet leading the detonation front is formed in the channel. The

St. Petersburg Mechanical Institute. Translated from Inzhenerno-fizicheskii Zhurnal, Vol. 62, No. 2, pp. 261-266, February, 1992. Original article submitted April 19, 1991.